RAYTHEON 23' x 22' 50GHZ PULSE SYSTEM

Terry Speicher
Nearfield Systems, Incorporated
1330 E. 223rd Street, Bldg. 524
Carson, CA 90745
www.nearfield.com

Angelo Puzella and Joseph K. Mulcahey
Raytheon Electronic Systems
528 Boston Post Road
Sudbury, MA 01776
angelo_puzella@res.raytheon.com and Joseph_K_Mulcahey@res.raytheon.com

Abstract

Nearfield Systems, Inc. in Carson, California delivered a vertical 23' by 22' (7.0m x 6.7m) near-field test range to Raytheon Electronic Systems in Sudbury, Massachusetts. This planar and cylindrical measurement system is capable of characterizing antennas of various physical sizes in continuous wave or in pulse mode from 800MHz to 50GHz. The near-field measurements are computer controlled and capable of multiple frequency, multiple beam and multiple polarization in AUT transmit or receive modes. The precision robotic system uses a Data Acquisition Controller running NSI software to provide four-axes for probe positioning and three-axes for antenna positioning. The RF subsystem is based on the HP 8530A microwave receiver, HP 83630B RF source, HP 83621A LO source and HP 85309A LO/IF Distribution Unit. The test range was evaluated using the NIST 18-term error analysis on a 45GHz 54" diameter left-hand circular polarized reflector antenna.

Keywords: Antenna measurements, Facility descriptions, Measurement errors, Near-field scanners, Planar near-field, Range evaluation.

1. Introduction

Nearfield Systems, Inc. delivered a turnkey antenna measurement system to Raytheon Electronic Systems in Sudbury, MA. The system supports both planar and cylindrical near-field antenna measurements and will be used to characterize a variety of antennas with apertures up to 6m over a frequency range of 0.8GHz to 50GHz. The system is housed in a new facility that was designed especially for the system. The anechoic chamber is lined with 18-inch pyramidal cone absorber on the walls, floor and ceiling. An azimuth/elevation/azimuth positioner stage is mounted on a linear slide that is recessed below floor level. The positioner is used to align the antenna for planar near-field scans and to rotate the AUT during cylindrical scanning. The motorized slide positioner allows the AUT to be translated in the Z axis dimension (normal to the scan plane).

The near-field system allows a full 23 feet of horizontal (X-axis) travel and 22 feet of vertical (Y-axis) travel for planar near-field scanning and a full 360° by 22 feet for cylindrical near-field scanning. The dual measurement capability of the system permits accurate characterization of both narrow and fan beam antennas.

2. System Overview

As shown in Figure 2.1, the XY scanner is located at the end of the anechoic chamber permitting full access to the AUT. The system provides seven axes of motion: X, Y, Z, probe polarization (NSI supplied four), AUT Z-stage, and azimuth/elevation positioner (Raytheon supplied three). The scanner base rails are constructed on dual granite beams for accuracy and thermal stability. The scanner also includes an optical measurement package for precise determination of linear distance and positioning error. Measured errors are used to correct the probe position while scanning. With laser feedback, the positioning error is <0.05mm RMS or less for both the X- and Y-axes. Using the

NSI structure monitor capability, planarity of the scan plane is correctable to within 0.05mm RMS. An overview of system capabilities is shown in Table 2.1.

The NSI Data Acquisition Controller (DAC) is capable of cross-axis correction to improve overall scanner accuracy and planarity during the antenna measurement acquisition process. The patented laser system detects and corrects for small mechanical variations in the horizontal X rails that will cause the vertical tower to tilt in both the Z and X axis as it is moved along the X-axis. The correction system will dynamically compensate for tower deflection errors by adjusting the timing triggers to compensate for X axis tilt and adjusting a Z translation stage during scanner motion. This technique ensures data is spatially accurate thereby reducing or eliminating the need to apply post acquisition software error correction. Rotation and Z-translation stages for the probe are also part of the scanner.

3. RF Subsystem

The RF subsystem is based on the HP 8530A microwave receiver, HP 83630B RF source, HP 83621A LO source and HP 85309A LO/IF Distribution Unit. The system supports CW and pulsed antenna measurements from 0.8GHz to 50GHz using frequency multipliers for operation above 26.5GHz. The system is capable of multiplexing up to eight AUT beams and two probe polarizations. The HP 8530A receiver provides accurate amplitude and phase measurements at a maximum rate of 2500 points per second. The HP 83630B and HP 83621B sources can switch frequencies at a rate of approximately 8msec. The SP8T AUT PIN switch and the SP2T probe PIN switch have switching speeds of approximately 1μsec.

RF subsystem setup, timing and control are performed by the NSI software running on the NSI acquisition computer. The NSI software also controls the scanner, and performs all data processing functions.

The RF subsystem is fully reciprocal and supports both transmit and receive from the AUT. Figure 3.1 shows the AUT transmit mode when the RF energy is being transmitted by the AUT with the probe receiving the RF energy. AUT transmit mode requires manual reconfiguration so that the RF multiplier module is located near the AUT and connected to one of the two reference mixers located near the AUT. AUT receive mode requires manual reconfiguration so that the RF multiplier module is located on the probe carriage and connected to one of the two test mixers located on the probe carriage.

When pulsed mode testing is used, the software is set to enable pulse mode over all frequency ranges. The operator has full control over the pulse repetition frequency, pulse width and power.

4. Test Results

This section provides a description of the antenna test results that contribute significant uncertainty values in the NIST 18-term error assessment. The parameters of interest were the on-axis gain, the relative sidelobe and the cross polarization level.

The antenna used for range assessment tests was a 54” diameter reflector antenna operating at 45GHz mounted as shown in Figure 4.1. The polarization is left hand circular. The test objectives were to evaluate the total measurement system errors for gain, sidelobes and cross polarization and to determine the magnitude of the individual error sources. Sixty-one data files were acquired as part of the range assessment process. Figures 4.2 and 4.3 are the computed far-field patterns for the antenna under test.

Numerous NIST terms for this particular antenna do not contribute significant errors as listed in Table 4.1. The insignificant values are: term #1 probe relative pattern, term #2 probe polarization ratio, term #4 probe alignment error, term #7 AUT alignment error, term #9 measurement area truncation error, term #10 probe X and Y position error, term #14 systematic phase error, term #15 receiver dynamic range, term #17 leakage and crosstalk and term #18 random amplitude and phase error.

Probe gain measurement is NIST term #3. The probe used as part of this assessment was an uncalibrated open-ended waveguide. An analytic model that is built into the NSI software estimates its gain. The gain accuracy shown in the table is based on using a calibrated probe that would be installed for production measurements. A calibrated probe was not available at the time of tests.

Normalization constant is NIST term #5. This term is estimated by using the receiver linearity test results to determine receiver error, analyzing

the method used to determine transmission line losses, and measuring changes due to cable flexing. Typical estimates of uncertainty are included in Table 4.1 assuming that the AUT input and probe output terminals are connected directly together without using a substitution cable.

Impedance mismatch error is NIST term #6. This term is computed using Reflection Coefficient magnitudes for the probe, AUT, the generator, and the load as shown in Table 4.1. A predicted impedance mismatch error of 0.10dB was used.

Data point spacing is NIST term #8. Because of the extremely narrow beamwidth of the AUT, the primary region of interest was within 15 degrees of the main beam. The narrow beam provides an effective band limit that allows measurements at approximately λ rather than $\lambda/2$. Using measurements at λ and $\lambda/2$, far-field patterns were compared and computed relative to its own peak value. Errors in relative quantities such as sidelobe and polarization ratio are correctly represented. The gain error is not derived from the E/S level, but is obtained from noting the changes in the peak value due to each error test. All of the tests for the other error sources were performed using data with a near-field spacing of λ. The values for this term are shown in Table 4.1.

Probe Z position error is NIST term #11. The z-position errors measured during installation and ATP testing provide the input data to estimate δ_z for each sidelobe region. These planarity measurements as a function of probe X and Y position were made with reference to a vertical reference plane, and part of the z-error is due to a linear variation as a function of Y due to a small tilt of the Y-rails. The values for this term are shown in Table 4.1.

Mutual coupling between the probe and the AUT is NIST term #12. The error for this term is determined by comparing a pattern taken at one z-position to a pattern where two or more z-positions have been averaged together. Table 4.1 shows results of the measurements and analysis using five z-positions.

The receiver amplitude linearity is NIST term #13. Since the HP receiver error is difficult to measure, the NSI software can simulate the effect of the receiver non-linearity by applying amplitude offsets corresponding to modeled non-linearity curves. The errors are determined by subtracting the resulting pattern from the original. The difference pattern shows a characteristic change in the main beam width and very little effect on the sidelobe or cross-polarized levels. The simulated results were compared to actual measurements by taking measurements with decreasing input power levels. As the power level was changed, the averaging was also increased to maintain an approximate constant signal to noise ratio so changes would not be due to dynamic range differences. The values of a comparison between the 0 and -6dB input levels are shown in Table 4.1.

Room scattering is NIST term #16. This error is determined by pattern comparison. The first pattern is measured at an initial probe z-position and is compared to a pattern where both the probe and the AUT are moved in Z. Measurements were made with the AUT and the probe moved from the initial z=0 position to z= 5.85 inches. Subtracting the resulting far-field patterns gives a measure of the room scattering. The values for this term are shown in Table 4.1.

5. Range Summary

A 45GHz LHCP 54” diameter antenna was used to evaluate the Raytheon 23' x 22' near-field measurement range for planar near-field scans. The results of the study predict a gain error of 0.23dB and a sidelobe error of 2.0dB when using a calibrated probe.

6. References

1. Demas, J. and Speicher, T., "Innovative Mechanical Designs For Scanners," *AMTA Symposium,* pp 366-371, November 1997.

2. Newell, A. C., ”Error Analysis Techniques For Planar Near-Field Measurements,” *IEEE Trans. Antennas Propagation*, Vol. 36, No. 6, pp 754-767, June 1988.

3. Slater, Dan, *Nearfield Antenna Measurements.* Artech House 1991.

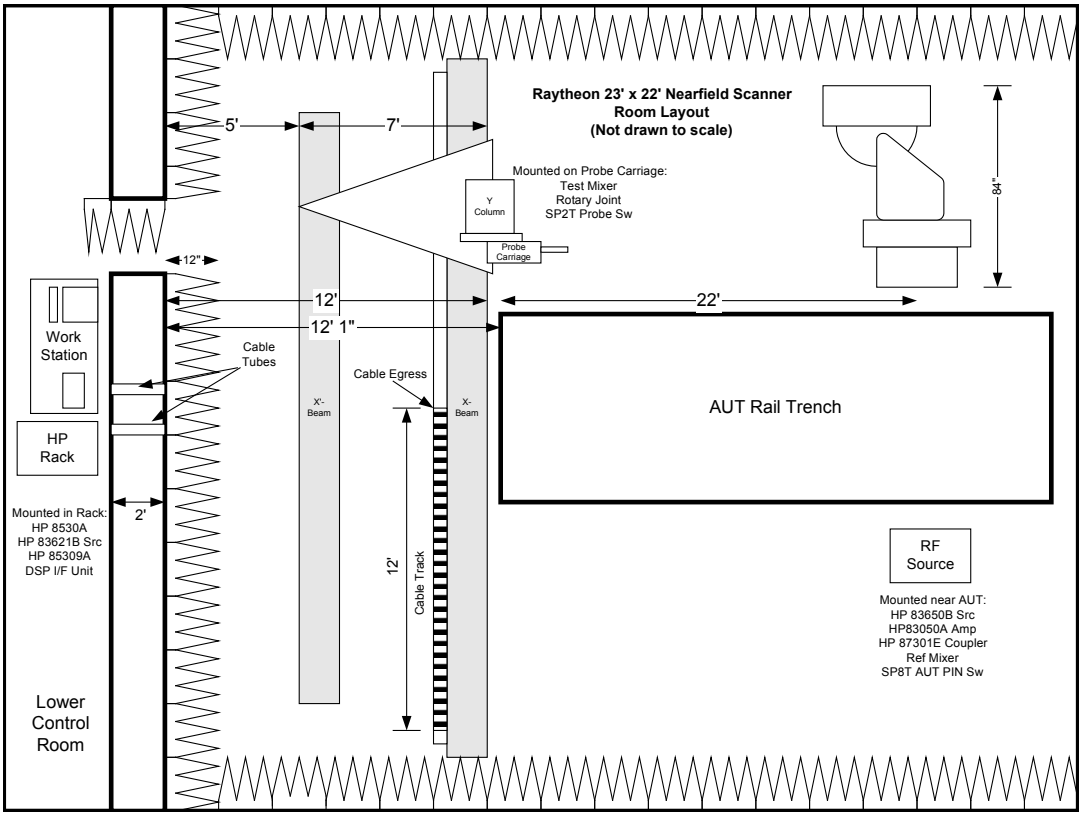

Figure 2.1 Raytheon 23' x 22' Near-field Range Layout

Parameter	Specification
Scan Plane Area	7m x 6.7m (23’ x 22’)
Frequency Range	0.8 – 50 GHz planar and cylindrical
Scan Plane Orientation	Vertical
X-position error (corrected)	0.05 mm rms
X-position repeatability	0.025 mm
X-position resolution	0.025 mm
X-axis travel	7.0m (23')
X-axis speed (max)	250 mm/s
Y-position error (corrected)	0.05 mm rms
Y-position repeatability	0.025 mm
Y-position resolution	0.025 mm
Y-axis travel	6.7m (22’)
Y-axis speed (max)	375 mm/s
Planarity (rms) corrected	0.05 mm rms
Z-axis repeatability	0.025 mm
Z-axis resolution	0.025 mm
Z-axis travel	0.25 m
Z-axis speed (max)	25 mm/s
Pol-axis load capacity	20 kg
Pol-axis position error	0.02 deg
Pol-axis repeatability	0.01 deg
Pol-axis resolution	0.01 deg
Pol-axis travel	360 deg
Pol-axis speed (max)	40 deg/s

Table 2.1 System Capability Overview

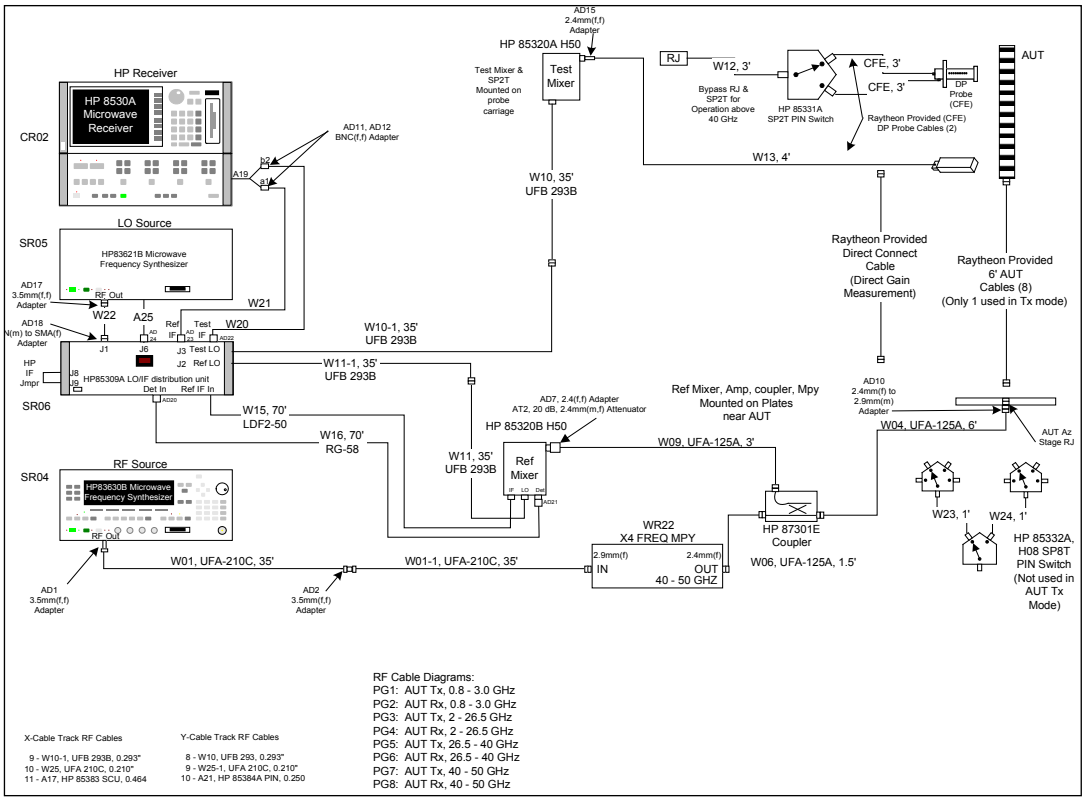

Figure 3.1 AUT 40 to 50GHz Transmit Mode RF Cable Diagram

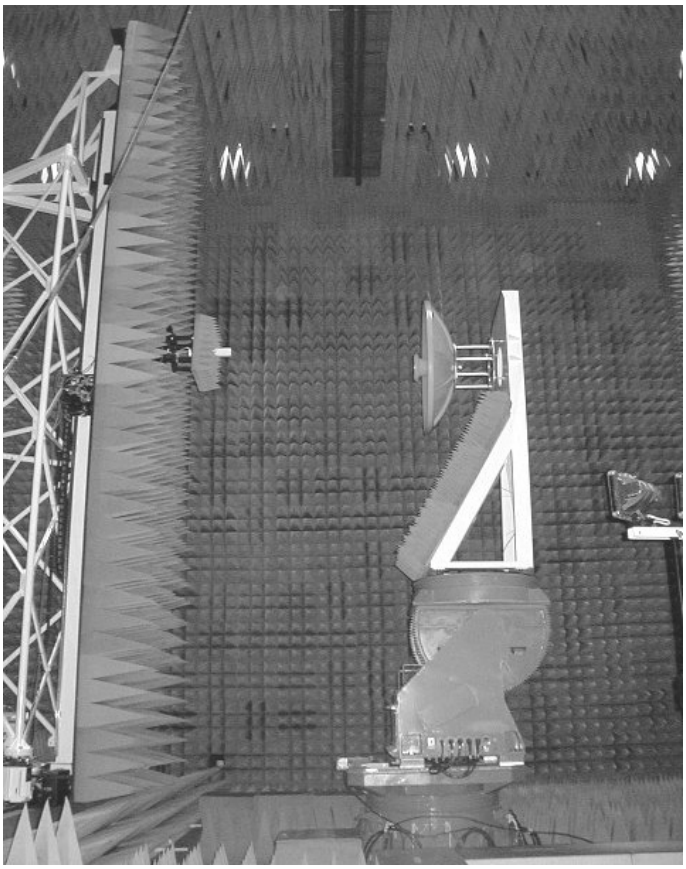

Figure 4.1 7.0m x 6.7m Vertical NF Scanner Testing 54" Reflector Antenna

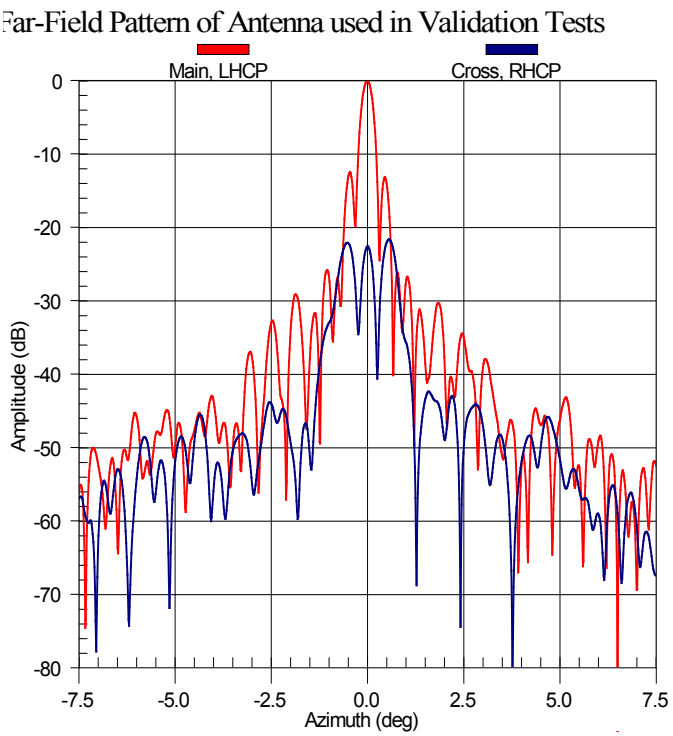

Figure 4.2 H-Cut Far-field pattern of antenna through beam peak.

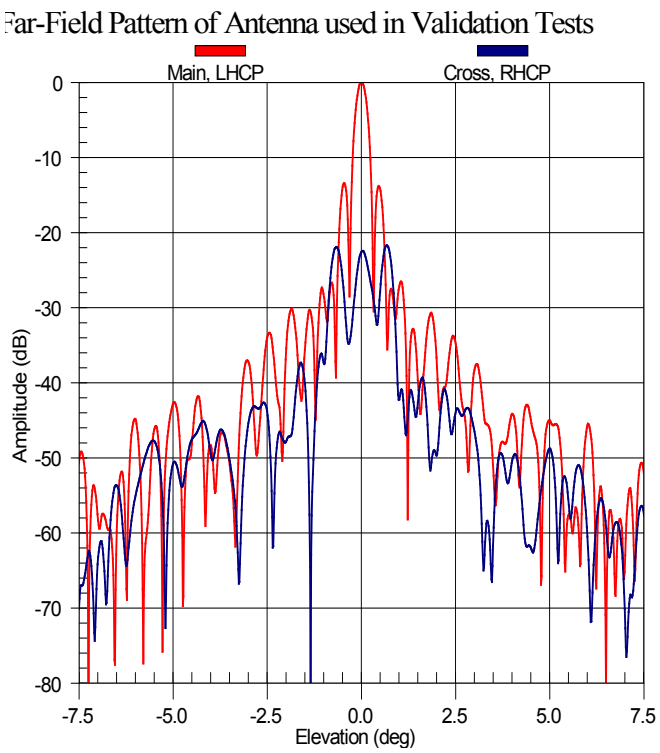

Figure 4.3 V-Cut Far-field pattern of antenna through beam peak.

#	Item	Gain Error (dB)	-30dB Sidelobe Error (dB)	On Axis Cross Polarization Error (dB)
1	Probe relative pattern	0.00	0.01	0.00
2	Probe polarization ratio	0.00	0.00	0.45
3	Probe gain measurement	0.10	0.00	0.00
4	Probe alignment error	0.00	<0.001	0.00
5	Normalization constant	0.15	0.00	0.00
6	Impedance mismatch error	0.10	0.00	0.00
7	AUT alignment error	0.00	0.00	0.00
8	Data point spacing (aliasing)	0.02	0.15	0.80
9	Measurement area truncation	0.003	0.30	0.09
10	Probe Y position errors	0.002	0.01	0.004
11	Probe Z position error	0.02	1.60	0.04
12	Mutual coupling (Probe/AUT)	0.05	0.10	0.80
13	Receiver amplitude linearity	0.05	0.15	1.30
14	Systematic phase error	0.004	0.09	0.09
15	Receiver dynamic range	0.01	0.15	0.30
16	Room scattering	0.04	1.00	0.80
17	Leakage and crosstalk	0.04	0.53	0.67
18	Random amplitude/phase errors	0.003	0.09	0.04
	Total (rss)	0.23	2.0	2.1

Table 4.1 Raytheon 45GHz Antenna NIST Error Budget